DØ Note 4349-Conf - Version 2.1 - FINAL

Search for Large and TeV^{-1} Extra Dimensions in the Dielectron Channel with 200 pb^{-1} of Data

The DØ Collaboration
URL: http://www-d0.fnal.gov

(Dated: March 17, 2004)

We report preliminary results on search for large and TeV^{-}1 spatial extra dimensions in the dielectron channel using $\sim$ 200 pb^{-1} of data collected by the DØ Experiment at the Fermilab Tevatron in 2002-2003 (Run II). The search for TeV^{-1} extra dimensions is the first experimental search of a kind. The data are in excellent agreement with Drell-Yan production and do not exhibit any evidence for new physics beyond the Standard Model, so we use them to set limits on large and TeV^{-1} extra dimensions. A lower limit on the compactification scale of TeV^{-1} extra dimensions of 1.12 TeV has been set. While inferior to indirect limits from precision measurements, these limits are complementary and reflect the first dedicated search for TeV^{-1} extra dimensions at colliders. We also extract limits on the fundamental Planck scale in the model with large extra dimensions.

Preliminary Results for Winter 2004 Conferences

I. INTRODUCTION

That we live in a three-dimensional space may seem to be a well-known fact; however it lacks rigorous experimental proof. Recent advances in string theory suggest that there might exist hidden dimensions in space of a finite size R beyond the three we sense daily. More recently, in 1998, an attractive realization of the above idea has been proposed by Arkani-Hamed, Dimopoulos, and Dvali [1] (ADD). In their formulation, the standard model (SM) particles are confined to a 3-dimensional membrane (D3-brane), as expected in the string theory, and SM gauge interactions are therefore restricted to this brane. At the same time, gravity is allowed to propagate in the n extra spatial dimensions, which explains its apparent weakness. Fundamentally, gravity is as strong as other gauge forces, but this becomes apparent only for a $(3+n)$-dimnesional observer. The apparent Planck scale of $M_{\rm Pl} = 1/\sqrt{G_N} \sim 10^{19}$ TeV $\gg M_{\rm EW} \sim 1$ TeV merely reflects its volume supression due to the dilution in extra space.

Assuming that the fundamental, $(3+n)$-dimensional Planck scale, M_S, is in the TeV range, suggests for $n = 1$ a very large $R \sim 10^8$ km (of the size of our solar system), which is ruled out by the known $1/r^2$ dependence of the gravitational force at large distances. However, for $n \geq 2$ the expected R is less than 1 mm, and therefore does not contradict existing gravitational experiments. For instance, for $n = 2$ we have $R \sim 1$ mm. For larger n, compactification radius drops as a power law (*e.g.*, ~ 3 nm for $n = 3$). Thus $n = 2$ is the minimum number of these, *large* extra dimensions (ED).

Another interesting model was also proposed [2, 3], in which matter resides on a p-brane ($p > 3$), with chiral fermions confined to the ordinary three-dimensional world internal to the p-brane and the SM gauge bosons also propagating in the extra $\delta > 0$ dimensions internal to the p-brane. (Gravity in the bulk is not of direct concern in this model.) It was shown [2] that in this scenario it is possible to achieve the gauge coupling unification at a scale much lower than the usual GUT scale, due to a much faster power-law running of the couplings at the scales above the compactification scale of the extra dimensions. The SM gauge bosons that propagate in the extra dimensions compactified on S^1/Z_2, in the four-dimensional point of view, are equivalent to towers of Kaluza-Klein states with masses $M_n = \sqrt{M_0^2 + n^2/R^2}$ $(n = 1, 2, ...)$, where $R = M_C^{-1}$ is the size of the compact dimension, M_C is the corresponding compactification scale, and M_0 is the mass of the corresponding SM gauge boson.

There are two important consequences of the existence of the KK states of the gauge bosons in collider phenomenology. (i) Since the entire tower of KK states have the same quantum numbers as their zeroth-state gauge boson, this gives rise to mixings among the zeroth (the SM gauge boson) and the nth-modes $(n = 1, 2, 3, ...)$ of the W and Z bosons. (The zero mass of the photon is protected by the $\mathrm{U(1)_{EM}}$ symmetry of the SM.) (ii) In addition to direct production and virtual exchanges of the zeroth-state gauge bosons, both direct production and virtual effects of the KK states of the W, Z, γ, and g bosons would become possible at high energies.

In this paper, we study the effects of virtual exchanges of the KK states of the Z and γ in high energy $p\bar{p}$ collisions at the Fermilab Tevatron.

II. THEORY

A. Effects of Virtual KK States

For Drell-Yan production of a pair of leptons, the amplitude squared for $q\bar{q} \to \ell^+\ell^-$ or $\ell^+\ell^- \to q\bar{q}$ (without averaging over the initial spins or colors) is given by:

$$\sum |\mathcal{M}|^2 = 4u^2 \left(|M_{\rm LL}^{\ell q}(s)|^2 + |M_{\rm RR}^{\ell q}(s)|^2 \right) + 4t^2 \left(|M_{\rm LR}^{\ell q}(s)|^2 + |M_{\rm RL}^{\ell q}(s)|^2 \right) ,$$

where, for the compactification scale $M_C \gg \sqrt{s}, \sqrt{|t|}, \sqrt{|u|}$:

$$M_{\alpha\beta}^{\ell q}(s) = e^2 \left\{ \frac{Q_\ell Q_q}{s} + \frac{g_\alpha^\ell g_\beta^q}{\sin^2\theta_W \cos^2\theta_W} \, \frac{1}{s - M_Z^2} - \left(Q_\ell Q_q + \frac{g_\alpha^\ell g_\beta^q}{\sin^2\theta_W \cos^2\theta_W} \right) \, \frac{\pi^2}{3M_C^2} \right\} . \tag{1}$$

The differential cross section, including the contributions from the KK states of the photon and Z, is given by [4]

$$\frac{d^2\sigma}{dM_{\ell\ell}dy} = K \frac{M_{\ell\ell}^3}{72\pi s} \sum_q f_q(x_1) f_{\bar{q}}(x_2) \, \left(|M_{LL}^{eq}(\hat{s})|^2 + |M_{LR}^{eq}(\hat{s})|^2 + |M_{RL}^{eq}(\hat{s})|^2 + |M_{RR}^{eq}(\hat{s})|^2 \right) ,$$

where $M_{\alpha\beta}^{eq}$ is given by Eq. (1), $\hat{s} = M_{\ell\ell}^2$, $\sqrt{s}$ is the center-of-mass energy in the $p\bar{p}$ collisions, $M_{\ell\ell}$ and y are the invariant mass and the rapidity of the lepton pair, respectively, and $x_{1,2} = \frac{M_{\ell\ell}}{\sqrt{s}} e^{\pm y}$. The variable y is integrated numerically to obtain the invariant mass spectrum. The QCD K-factor is given by $K = 1 + \frac{\alpha_s(\hat{s})}{2\pi} \frac{4}{3} (1 + \frac{4\pi^2}{3}) \approx 1.3$ [5].

It is clear from the above equation that it's bilinear in the following parameter, dependent on the compactification scale of the TeV^{-1} extra dimension:

$$\eta_C = \frac{\pi^2}{3M_C^2} \tag{2}$$

We use these matrix elements in the Monte Carlo generator of Ref. [4, 6] to simulate the effects of virtual KK states of the Z and γ. Since the functional form of the cross section is a bilinear form in η_C, we apply directly all the fitting apparatus developed in Ref. [6] with a straightforward replacement of $\eta_G \to \eta_C$.

B. Current Limits on M_C

Table I summarizes current limits on the compactification scale based on phenomenological analysis of the available data. Note that there has been no dedicated experimental search for TeV^{-1} extra dimensions as of yet.

TABLE I: Best-fit values of $\eta_C = \pi^2/(3M_C^2)$ and the 95% C.L. upper limits on η_C for individual data set and combinations. Corresponding 95% C.L. lower limits on M_C are also shown. From Ref. [4].

	η_C (TeV^{-2})	η_{95} (TeV^{-2})	M_C^{95} (TeV)
LEP 2:			
hadronic cross section, ang. dist., $R_{b,c}$	$-0.33\ ^{+0.13}_{-0.13}$	0.12	5.3
μ, τ cross section & ang. dist.	$0.09\ ^{+0.18}_{-0.18}$	0.42	2.8
ee cross section & ang. dist.	$-0.62\ ^{+0.20}_{-0.20}$	0.16	4.5
LEP combined	$-0.28\ ^{+0.092}_{-0.092}$	0.076	6.6
HERA:			
NC	$-2.74\ ^{+1.49}_{-1.51}$	1.59	1.4
CC	$-0.057\ ^{+1.28}_{-1.31}$	2.45	1.2
HERA combined	$-1.23\ ^{+0.98}_{-0.99}$	1.25	1.6
TEVATRON:			
Drell-yan	$-0.87\ ^{+1.12}_{-1.03}$	1.96	1.3
Tevatron dijet	$0.46\ ^{+0.37}_{-0.58}$	1.0	1.8
Tevatron top production	$-0.53\ ^{+0.51}_{-0.49}$	9.2	0.60
Tevatron combined	$-0.38\ ^{+0.52}_{-0.48}$	0.65	2.3
All combined	$-0.29\ ^{+0.090}_{-0.090}$	0.071	6.8

III. SEARCH FOR LARGE AND TEV^{-1} EXTRA SPATIAL DIMENSIONS IN THE DIELECTRON CHANNEL

The data used for this analysis was selected using all the available recent data from DØ Run II, i.e. data taken between April 2002 and November 2003. All the data have been reconstructed with the DØ reconstruction program (`d0reco`) version p14. These data correspond to the total intergrated luminosity of approximately 198 ± 13 pb^{-1} . For the detail of the preselection, see Ref. [6].

There are two modifications that have been introduced at the final stages of selection:

- In order to ensure that we select dielectron final states, we require at least one of the EM cluster to have a matching track, with the spatial match probability > 0.01. The efficiency of this selection is discussed below.
- Since the requirement of a matching track reduces QCD background dramatically, we remove the tracking isolation cut used in the diEM analysis, which allowed us to maximize the selection efficiency.

Using the Z-events, we obtained the following tracking efficiencies of the requirement of a single track to match one of the two EM objects:

$$\begin{aligned} \varepsilon^{\mathrm{tr}}_{\mathrm{CC-CC}} &= 0.96 \pm 0.01; \\ \varepsilon^{\mathrm{tr}}_{\mathrm{CC-EC}} &= 0.94 \pm 0.01; \\ \varepsilon^{\mathrm{tr}}_{\mathrm{EC-EC}} &= 0.84 \pm 0.01. \end{aligned} \tag{3}$$

The overall selection efficiencies for the three topologies are as follows:

$$\begin{aligned} \varepsilon_{\mathrm{CC-CC}} &= 0.74 \pm 0.02; \\ \varepsilon_{\mathrm{CC-EC}} &= 0.74 \pm 0.02; \\ \varepsilon_{\mathrm{EC-EC}} &= 0.66 \pm 0.02. \end{aligned} \tag{4}$$

The above selections reduce the analysis sample to 15,602 events, corresponding to 8,246 CC-CC, 5,949 CC-EC, and 1,407 EC-EC combinations. This is our final candidate sample used in the analysis. The event selection flow is detailed in Table II.

Cut	Number of events
Reconstructed Data	∼700 mln events
NP diEM Stream	∼ 2 mln events
Starting root-tuple sample after duplicate event removal	485K
≥ 2 EM objects w/ $E_T > 20$ GeV and χ^2 cut	39,604
$E_T^{EM} > 25$ GeV, EMF cut, track match	15,602 = 8,246 CC-CC + 5,949 CC-EC + 1,407 EC-EC

TABLE II: Event selection.

The QCD background is estimated via method of Ref. [6]. The Drell-Yan background is simulated with the signal Monte Carlo. Since the direct diphoton production is at least an order of magnitude less than Drell-Yan production even at high masses, background from direct diphotons with photon conversions is negligible. All other physics backgrounds that results in the dielectron final state are negligible as well.

We observe very good agreement between the data and the background in all three topologies. To quantify the agreement between the data and the background in the steeply-falling mass spectrum, we calculate the prediction for the background above certain mass cutoff and compare it with the data for a number of mass cutoffs. The results are summarized in Table III and shown in Figs. 1, 2. Note that the rising QCD background in the EC-EC combinations above 140 GeV is due to the opposite-hemisphere events, which kinematically can only populate the region of high invariant masses.

Minimum $M_{\mathrm{EM-EM}}$	Bck, CC-CC	N, CC-CC	Bck, CC-EC	N, CC-EC	Bck, EC-EC	N, EC-EC	Bck, total	QCD bck	Data
50 GeV	8196	8212	5953	5942	1390	1385	15539	1062	15539
100 GeV	544	562	629	622	111	121	1285	367	1305
150 GeV	64.2	62	100	76	52.7	45	218	125	183
200 GeV	22.8	18	26.6	15	36.4	29	86.1	53.7	62
250 GeV	10.0	10	9.0	5	20.0	13	39.4	25.3	28
300 GeV	4.8	4	3.4	3	8.9	7	17.4	10.5	14
350 GeV	2.6	2	1.3	2	3.7	5	7.8	4.3	9
400 GeV	1.5	1	0.6	1	1.8	1	3.9	2.0	3
450 GeV	0.9	1	0.4	0	0.8	1	2.0	1.0	2
500 GeV	0.5	0	0.2	0	0.3	1	1.0	0.5	1
520 GeV	0.4	0	0.1	0	0.2	0	0.7	0.3	0

TABLE III: Comparison between the data and expected background for events above certain diEM mass cutoffs. Middle two columns show the number of candidate events and predicted background above the ee mass listed in the first column. Note an additional systematic error of 10% on the background prediction, depending on the mass.

Note that the effect of TeV^{-1} ED is more convoluted than the effects of large ED (see Ref. [6]). While the latter results in an overall enhancement of the cross section at high masses, the former have two distinct feature: an enhancement at large masses similar to that for large ED, and a new effect: negative interference between the first KK state of the Z/γ and the SM Drell-Yan in between the Z mass and M_C. Therefore, one would expect a deficit of events at intermediate masses and an enhancement at high masses - quite distinct signature. Clearly, uncorrelated background fluctuations could mimic such an effect; therefore it is important to correctly account for the background shape and its systematics.

1. *Limits on TeV^{-1} Extra Dimensions*

Since the signal and background are very different in all the event topologies we extract limit by constructing likelihood functions for each topology and then properly combining them in the fit. Monte Carlo studies show that

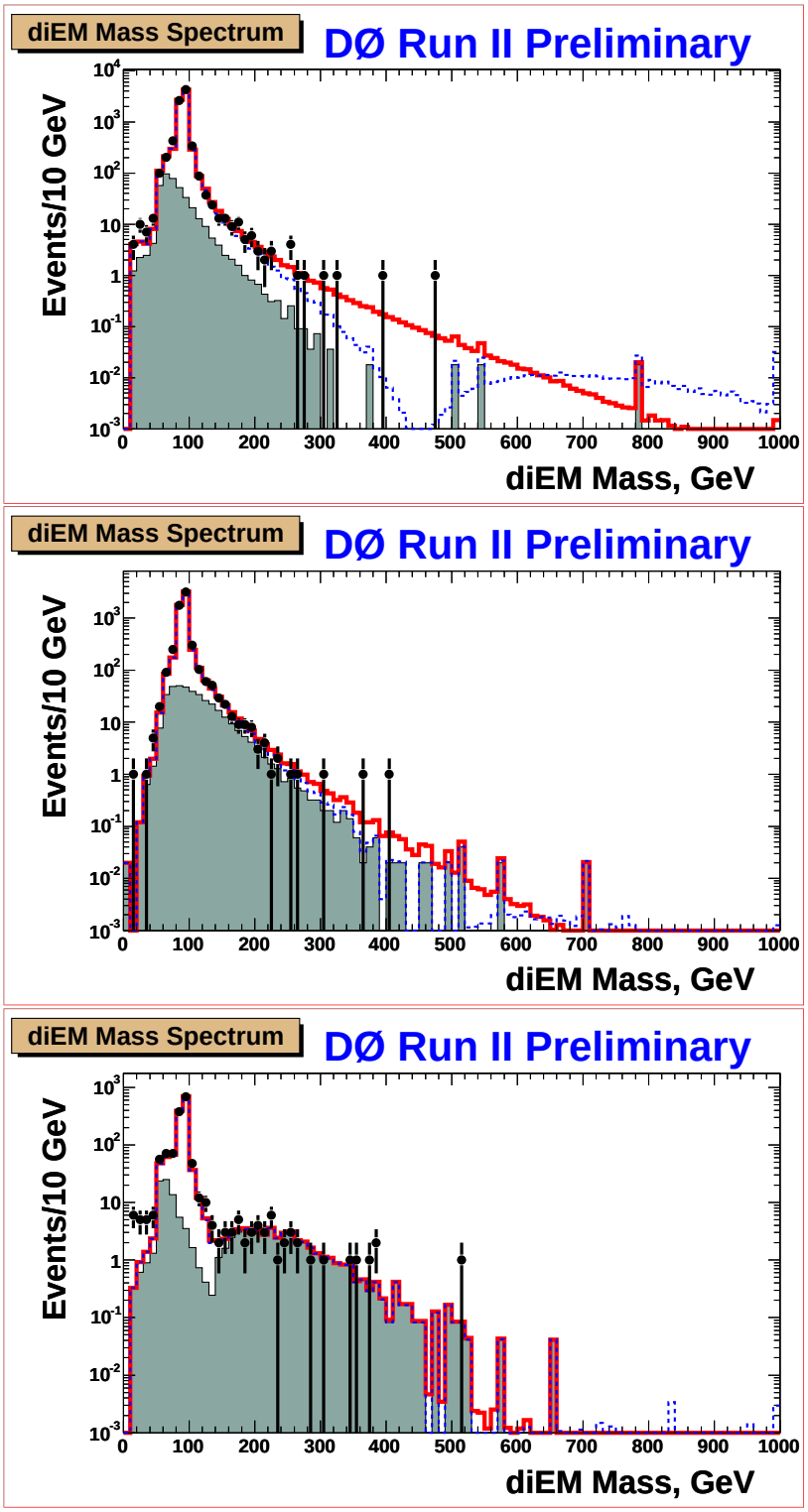

FIG. 1: The ee mass distribution for the base candidate sample. Points with the error bars are the data; light filled histogram represents the instrumental background from jets misidentified as EM objects; solid line shows the fit to the sum of the instrumental background and the SM predictions from Drell-Yan background. Top: CC-CC; middle: CC-EC; bottom: EC-EC. The dashed lines show the backgrounds plus a contribution from the TeV^{-1} signal with $\eta_C = 5.0\ \text{TeV}^{-2}$.

the large background in the EC-EC topology results in significant fluctuations of the best fit for the parameter η_C and thus dilutes the sensitivity for TeV^{-1} ED. (The situation is similar to the diEM search for large ED [6].) Therefore,

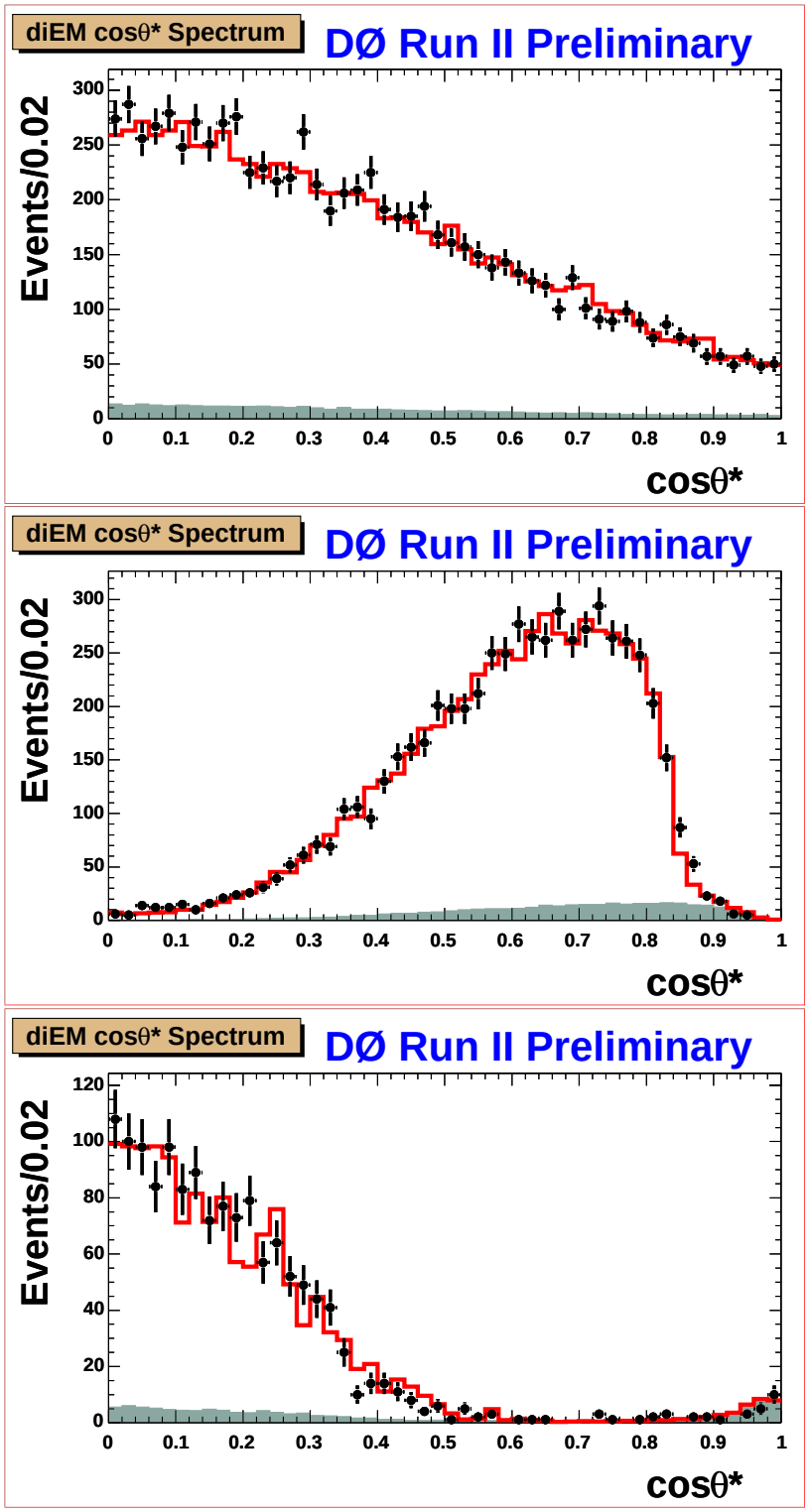

FIG. 2: The ee $\cos\theta^*$distribution for the base candidate sample. Points with the error bars are the data; light filled histogram represents the instrumental background from jets misidentified as EM objects; solid line shows the fit to the sum of the instrumental background and the SM predictions from Drell-Yan background. Top: CC-CC; middle: CC-EC; bottom: EC-EC.

we restrict ourselves to the CC-CC and CC-EC topologies. The 2D spectrum of the dielectron mass vs. the cosine of the scattering angle in the c.o.m. frame is shown in Fig. 3 for the data corresponding to these two topologies.

When setting limits on extra dimensions, we assign systematic uncertainties of 15% on signal and 10% on background

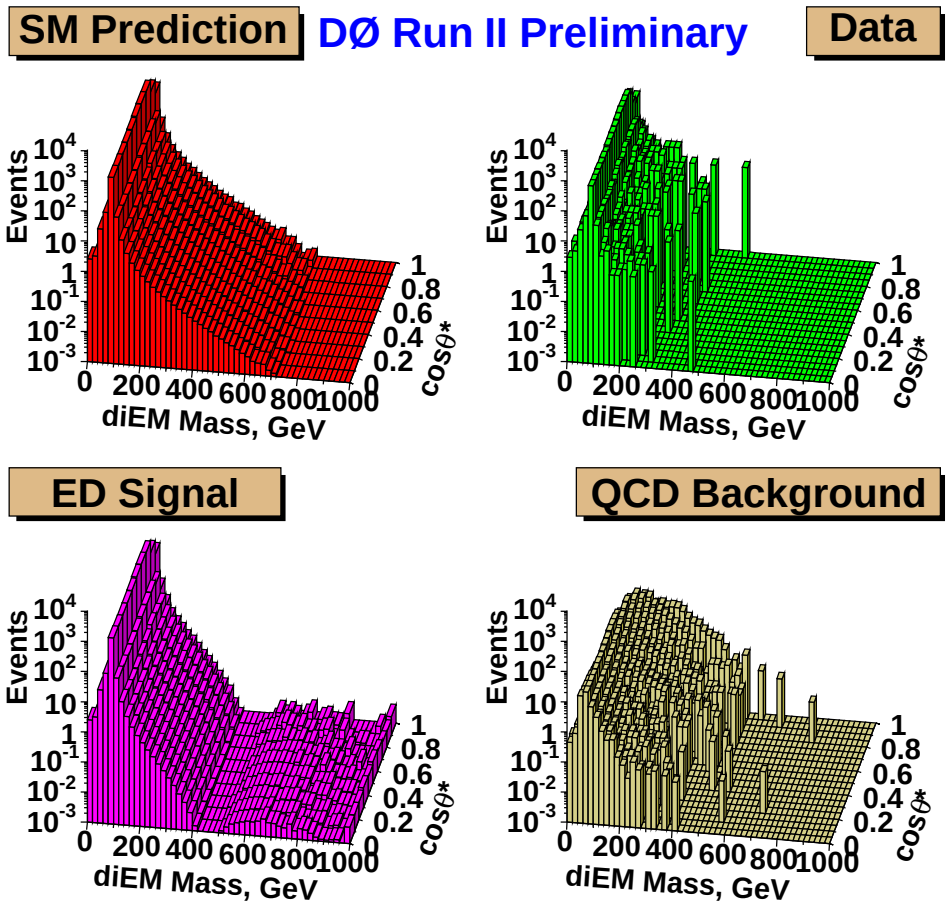

FIG. 3: The ee mass vs. $\cos\theta^*$ distribution for the combined CC-CC and CC-EC candidate samples. Top left: SM Drell-Yan background; top right: data; bottom left: TeV^{-1} ED signal plus the SM background for $\eta_C = 5.0$ TeV^{-2}; bottom right: instrumental background.

estimates, as documented in Table IV. The uncertainty on the signal is dominated by the uncertainty on the shape of the NLO corrections (i.e., energy dependence of the K-factor, 10%), possible residual E_T-dependence of the efficiency (5%), and uncertainty due to the choice of parton distribution functions. The 10% uncertainty in the background is due to the statistics and systematics of the instrumental background. The latter dominates only at high diEM masses, most sensitive to the effects of extra dimensions, and this is where the quoted uncertainty applies. At lower masses, the uncertainty on the background is dominated by the uncertainty on the product of integrated luminosity, selection efficiency, and the K-factor, which amounts to 7%.

Source of systematics	Uncertainty
K-factor	10%
Choice of p.d.f.	5%
Normalization to the Z	2%
E_T dependence of the efficiency	5%
Total	12%

TABLE IV: Sources of systematic uncertainty on the calculated differential cross section.

We then proceed with extracting the best estimate for parameter η_C by fitting two-dimensional distributions to the sum of the SM, interference, and the direct gravity templates. The size of the 2D-grid used in the main analysis in $M \times \cos\theta^*$ is 50×10. The results are stable w.r.t. the granularity of the grid. The best estimate on the parameter η_C from the fits are:

$$\eta_C = 0.90 \pm 0.97 \text{ TeV}^{-2}; \quad (5)$$

i.e. consistent with zero (no TeV^{-1} contribution), as expected. The 95% upper CL limit on η_C is set to be:

$$\eta_C^{95\%} = \begin{cases} 2.47 \text{ TeV}^{-2} & \text{Likelihood} \\ 2.63 \text{ TeV}^{-2} & \text{Bayesian} \end{cases} ; \tag{6}$$

The main reason Bayesian fit gives systematically higher values for the upper limit is that it includes proper background fluctuation. Unlike large extra dimensions, the TeV^{-1} models are more sensitive to the background as both negative and positive fluctuations affect the limits. We only use Bayesian fit when quoting limits. The obtained limits agree well with the expected sensitivity, based on a MC ensemble, see Fig. 4.

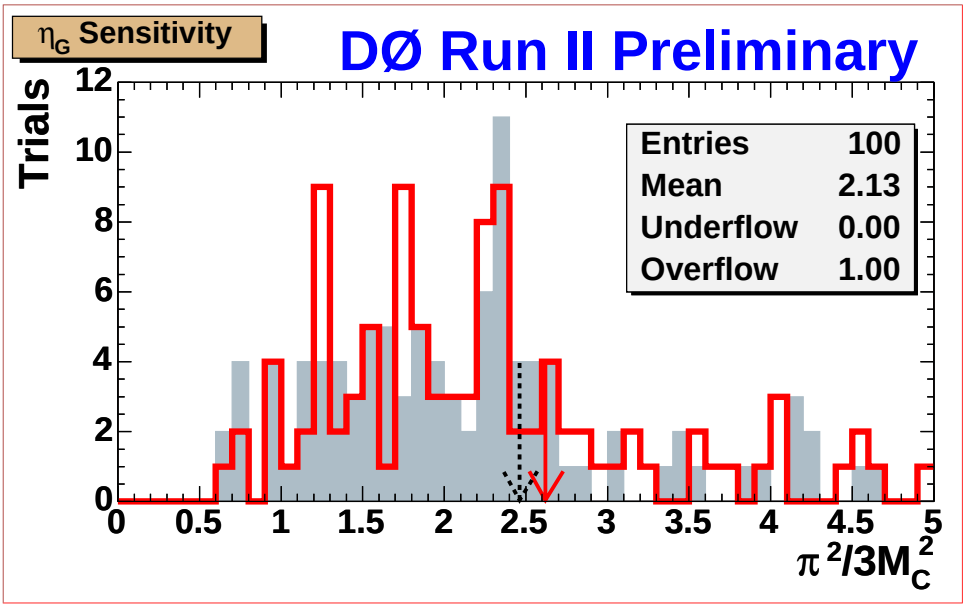

FIG. 4: Expected 95% CL upper limit on the parameter η_C from an ensemble of MC experiments, together with the actual limits obtained in this analysis. Shaded histogram: Bayesian limit; open histogram: Likelihood limit. The arrows indicate Bayesian (solid) and Likelihood (dashed) limits derived from data. Both the CC-CC and CC-EC combinations are used for the ensemble tests and in the actual limit from data.

We can transpate our final limit of $eta_C^{95} < 2.63$ TeV^{-2} into a lower limit on the compactification scale of the longitudinal extra dimension:

$$M_C > 1.12 \text{ TeV} \tag{7}$$

at the 95% confidence level. This is the final result of the analysis

2. *Interesting Candidate Events*

The invariant mass plots in all three topologies do not exhibit any interesting features or excesses. The highest mass dielectron event is the "event Callas" discussed in detail in Ref. [6]. The highest mass event in the spectrum is found in the EC-EC topology and is consistent with the background at $> 20\%$ confidence level. The parameters of these two highest mass events are listed in Table V. The event displays of the EC-EC candidate us shown in Fig. 5. This event has only one matching track and significant amount of missing transverse energy, which is consistent with the signature expected for a QCD background, the dominant background in this topology at high masses.

3. *Limits on Large Extra Dimensions*

For completeness, we also extract limits on Large extra dimensions from the dielectron sample. As expected, they are inferior to those from the combined dielectrons and diphotons. Straightforward fit to the CC-CC and CC-EC

Run	Event	$\not\!\!E_T$	Type	E_T^1 (p_T^1)	E_T^2 (p_T^2)	η_1	η_2	ϕ_1	ϕ_2	M	$\cos\theta^*$	$N_{\rm jet}$
162099	15851827	60.5	γe	86.6	39.3 (16)	-2.19	2.16	1.89	5.80	515	0.98	0
177851	28783974	8.8	e^+/e^-	239.2 (190.8)	226.9 (234.4)	-0.45	-0.50	0.48	3.68	475	0.01	1

TABLE V: Parameters of the two highest diEM mass candidates. Both events have only one reconstructed vertex, in a good agreement with the vertex from matching track(s). All energy variables are in GeV.

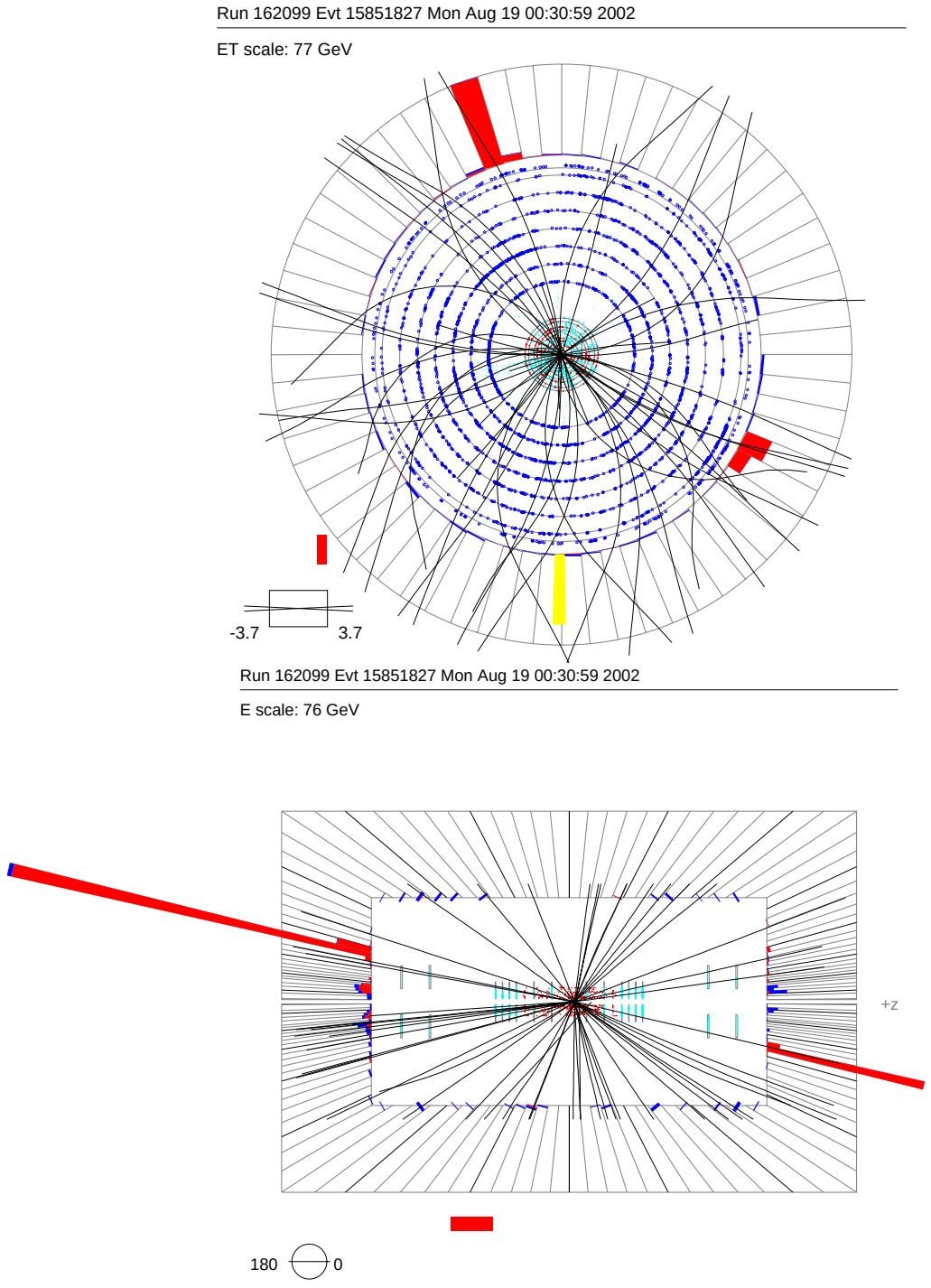

FIG. 5: Event display of the highest-mass ee candidate with the invariant mass of 515 GeV and $\cos\theta^*$ of 0.98 (Run 162099, Event 15851827).

combinations yields the following limit on the parameter η_G [6]:

$$\eta_G < 0.65 \text{ TeV}^{-4} \text{ at the 95\% CL}, \tag{8}$$

which corresponds to the limit of

$$M_S > 1.11 \text{ TeV}, \text{ at the 95\% CL} \tag{9}$$

in the GRW convention [7]. As expected, these limits are inferior to the ones obtained in the diEM analysis [6], but they are consistent with the expectations, as shown in Fig. 6.

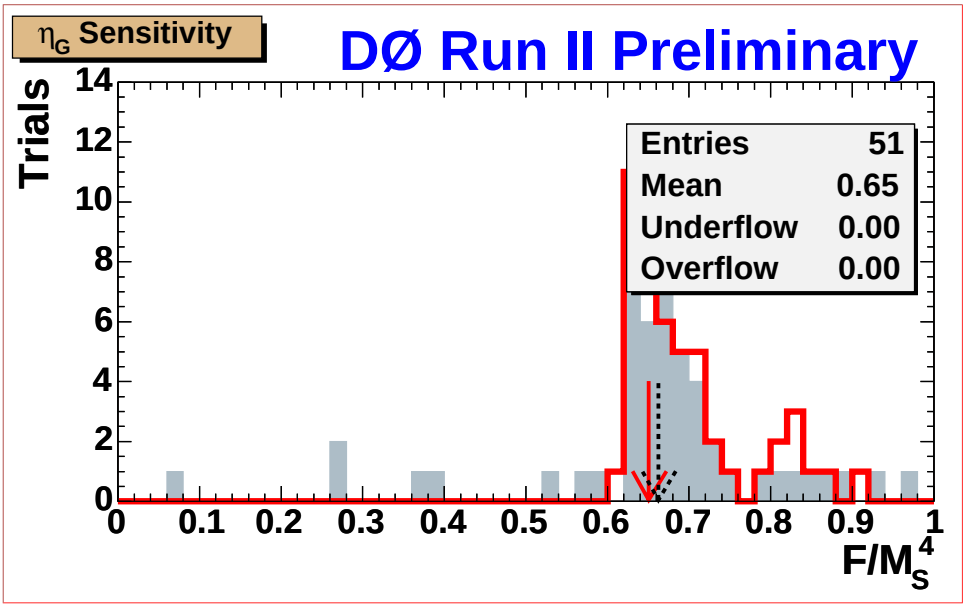

FIG. 6: Expected 95% CL upper limit on the parameter η_G from an ensemble of MC experiments, together with the actual limits obtained in this analysis. Shaded histogram: Bayesian limit; open histogram: Likelihood limit. The arrows indicate Bayesian (solid) and Likelihood (dashed) limits derived from data. Both the CC-CC and CC-EC combinations are used for the ensemble tests and in the actual limit from data.

IV. CONCLUSIONS

We performed search for large and TeV$^-1$ spatial extra dimensions in the dielectron channel using ~ 200 pb^{-1} of data collected by the DØ Experiment at the Fermilab Tevatron in 2002-2003 (Run II). The search for TeV^{-1} extra dimensions is the first experimental search of a kind. The data are in excellent agreement with Drell-Yan production and do not exhibit any evidence for new physics beyond the Standard Model, so we use them to set limits on large and TeV^{-1} extra dimensions. A lower limit on the compactification scale of TeV^{-1} extra dimensions of 1.12 TeV has been set. While inferior to indirect limits from precision measurements, these limits are complementary and reflect the first dedicated search for TeV^{-1} extra dimensions at colliders. We also extracted a lower limit of 1.10 TeV (in the GRW convention [7]) on the fundamental Planck scale in the model of large exra dimensions, less restrictive than the one set in our dombined diEM analysis [6]

[1] N. Arkani-Hamed, S. Dimopoulos, G. Dvali, Phys. Lett. **B429**, 263 (1998); I. Antoniadis, N. Arkani-Hamed, S. Dimopoulos, and G. Dvali, Phys. Lett. **B436**, 257 (1998); N. Arkani-Hamed, S. Dimopoulos, G. Dvali, Phys. Rev. D **59**, 086004 (1999); N. Arkani-Hamed, S. Dimopoulos, J. March-Russell, SLAC-PUB-7949, e-Print Archive: hep-th/9809124.
[2] K. Dienes, E. Dudas, and T. Gherghetta, Nucl. Phys. **B537**, 47 (1999).
[3] A. Pomarol and M. Quirós, Phys. Lett. **B438**, 255 (1998); M. Masip and A. Pomarol, Phys. Rev. D **60**, 096005 (1999); I. Antoniadis, K. Benakli, and M. Quirós, Phys. Lett. **B460**, 176 (1999).
[4] K. Cheung and G. Landsberg, Phys. Rev. D **65**, 076003 (2002).
[5] R. Harnberg, W.L. Van Neerven, and T. Matsura, Nucl. Phys. B**359**, 343 (1991).
[6] DØ Collaboration, DØ Note 4336-Conf, `http://www-d0.fnal.gov/Run2Physics/WWW/results/NP/NP01.pdf`.
[7] G. Giudice, R. Rattazzi, and J. Wells, Nucl. Phys. **B544**, 3 (1999), and revised version hep-ph/9811291.